IMPACT WELDING OF ALUMINUM TUBE TO A STAINLESS STEEL TARGET – EFFECT OF DEFORMATION OF TUBE ON BONDING CONDITION -

H. DATE
Department of Mechanical Engineering
Tohoku Gakuin University
1-13-1 Chuo, Tagajo 985-8537, Japan

ABSTRACT

A tubular aluminum projectile, subjected to a longitudinal impact, was impact-welded onto a stainless steel target using a gas gun at impact velocities of 200 m/s or more. The bonded area was estimated using acoustic tomography. The microstructures and element distribution in the joint were analyzed by means of SEM and Energy dispersive X-ray spectroscopy. It appeared that the aluminum projectile was bonded to stainless steel target at an impact velocity from 200 to 300 m/s. The compound layer was observed at the joining interface of aluminum/stainless steel by SEM. The bonding strength of aluminum/stainless steel joint showed a maximum of 190 MPa at 230 m/s and decreased with lower impact velocity. The bonding strength at impact velocities of 220~ 240 m/s was stronger than fracture strength of the aluminum projectile.

KEYWORDS

tube impact-welding, aluminum/stainless steel joint, compound layer, bonding strength

INTRODUCTION

The bonding technique of a tube to a tube or a plate is one of important techniques in mechanical engineering. It has been reported previously by Date and others that a cylindrical projectile with a flat end subjected to a longitudinal impact was bonded to a target plate at impact velocities of 200 m/s or more using a gas gun [1]. A tube was also impact-welded on a flat target using the same gas gun [2]. However the bonding mechanism of the tube could not be deduced by the results of the bar, since the two deformation processes during impact were different. Here, the impact welding of an aluminum tube to a stainless steel target was carried out and the bonding mechanism was examined by the bonding area, deformation process, bonding strength and the compound layer at the joining interface. The differences of the bonding mechanisms of the bar and the tube were clarified with some of the points described above and the proper phenomena about the tube were found out in the experiment.

MATERIALS AND EXPERIMENT

The materials used were stainless steel plates (SUS304) having a diameter of 40 mm and a thickness 5 mm as the target and pure aluminum rods (A1050) having an outer diameter of 11 mm, inner diameter of 6 mm and length 20 mm as the projectile. The aluminum was annealed at 623 K for 3.6 ks. The impact face of target was polished using polishing paper having a mesh of 800 after grinding. An aluminum projectile collided with the stainless steel target at an impact velocity of 200 m/s or more using compressed nitrogen gas [1]. The impact welding was carried out in a vacuum chamber because the air compressed between the target and impact face of the projectile prevented welding. The impact velocity of the projectile was evaluated by a laser beam system. The bonding area was observed and measured using a scanning acoustic tomograph. The microstructure and element distribution in joining interface of the bonded specimen sliced to a thickness of about 3 mm were analyzed by means of SEM and energy dispersive X-ray spectroscopy (EDX). A tension test for measuring the bonding strength of the sliced specimen described above was carried out [1].

BONDED AREA AND DEFORMATION OF PROJECTILE

Two ultrasonic images of the bonded area are shown in Fig. 1 (a) and (b). The impact velocities are 274 m/s and 339 m/s, respectively. The central ring areas in Fig. 1 (a) and (b) are called the inner ring area. Since appearance of the outer ring area shown in Fig.1 (a) depends on the impact velocity as described later, the inner ring area is defined as the bonded area hereafter. The superimposition of a bonded area and a cross-sectional profile of the deformed projectile are given in Fig. 2. Figure 2 shows that the bonded area was not formed at the center of the impact face of the tube wall, but more to the inside. It was clarified that the outer ring area was formed by the folding of the outer wall of the tube because the inner diameters of the outer ring area were larger than the initial outer diameters of the tube. It is observed that the metal of the inner wall flowed in and piled up in the tube. An opening like a crack is observed along the deformed inner wall of the tube.

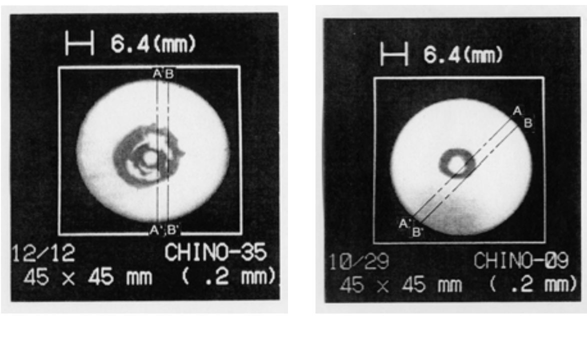

(a) v = 274 m/s (b) v = 339 m/s

Fig. 1 Acoustic images of bonded area

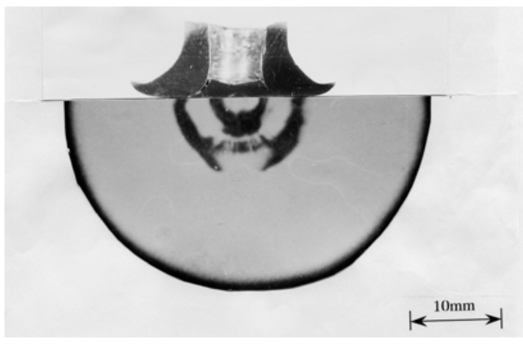

Fig. 2 Deformation profile of projectile and bonded area (v = 254 m/s)

The cross-sections of specimens bonded at the impact velocities of 238 m/s and 339 m/s are shown in Fig. 3(a) and (b). The contour of the outer wall after deformation is similar to the mushrooming profile. However, the profile of the inner wall is complicated as described below. Though the velocity of the metal flowing toward the center of the tube decrease as the inside of the tube is filled with the metal, the metal of the outer wall has continued to flow out during impact. The velocity difference of the two metal flows caused a crack to be initiated, grow and penetrate the wall. Finally the inside metal only is bonded at the target and the other part of the tube is separated from the target. It is clarified from Fig. 3 (a) and (b) that the outer ring area shown in Fig.1 (a) has vanished at a high velocity impact because the outer edge of the impact face of the projectile was lifted up from the target surface and the outer ring area was torn up. The effect of the impact velocity on the bonded area is given in Fig. 4. The size of the area hardly increases with impact velocity unlike the bar [1]. This means that the heat generation on the impact face of the tube is almost constant regardless of impact velocity.

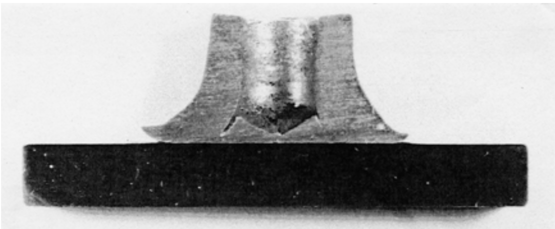

(a) v = 238 m/s

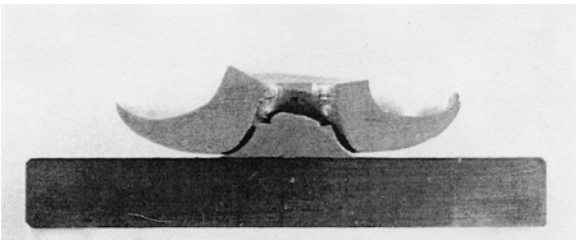

(b) v = 339 m/s

Fig. 3 Deformation process of projectile

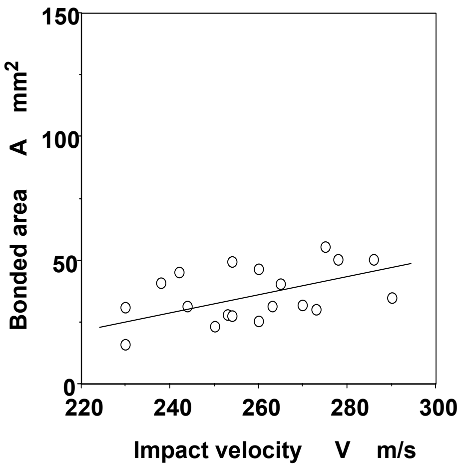

Fig. 4 Effect of impact velocity on bonded area

COMPOUND LAYER AND ELEMENT DISTRIBUTION

The magnified microstructure and X-ray image analysis of elements can be seen in Fig. 5 (a) and (b). Table I gives quantitative analysis of the phase formed at the joining interface in Fig. 5 (a). The maximum thickness of the compound layer was about 8 μm as seen in Fig. 5 (a) and (b). Figure 6 shows the maximum thickness of the compound layer plotted against impact velocities. The thickness hardly increases with impact velocity. The element distribution hardly depends on the position in the compound layer as shown in Table I and the content is almost constant regardless of impact velocity as shown in Fig. 7. The content of aluminum is more than that of Al_3Fe seen in the alloy phase diagram. The lack of dependence of aluminum content on the impact velocity and the position in the layer described above is the same as th

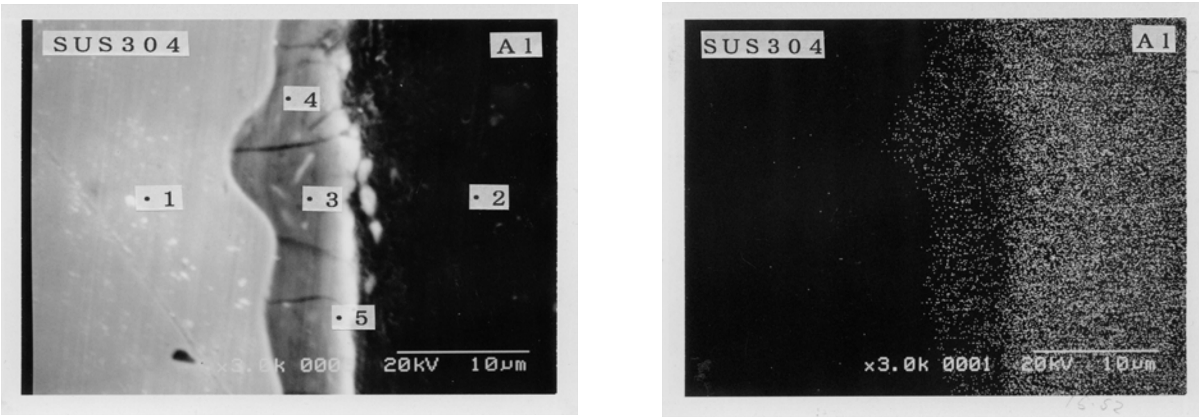

(a) Microstructure (b) X-ray image analysis of Al

Fig. 5 SEM and EDX images of compound layer

Table Ⅰ Quantitative analysis of elements (at %)

	1	2	3	4	5
Al	2.7	99.7	79.0	78.8	72.8
Cr	19.3	0.0	4.4	4.4	5.4
Fe	69,9	0.3	15.1	15.3	19.7
Ni	8.1	0.0	1.5	1.5	2.1

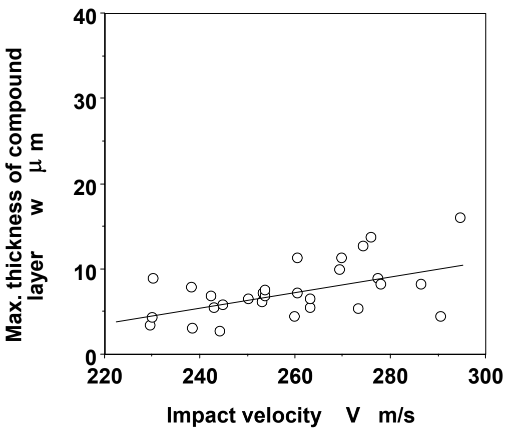

Fig. 6 Maximum thickness of compound layer plotted against impact velocity

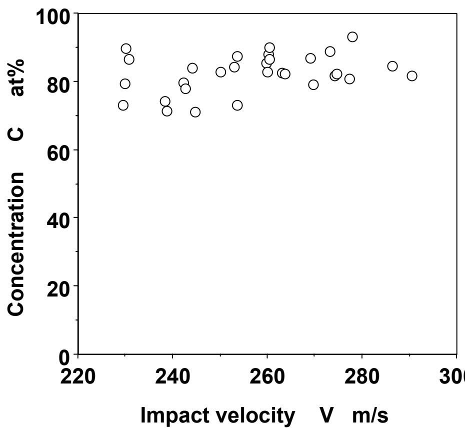

Fig.7 Effect of impact velocity on concentration of Al in compound layer

results for the bar [1]. A mechanical mixing model has been proposed previously by Date for interpreting the formation mechanism of the compound layer by impact welding [3]. The model consists of mixing and solidification of the melting metals. It is deduced from the results obtained using the model that the high content of aluminum in the layer shows much lower heat generation on the impact face than that of explosive welding.

BONDING STRENGTH

Figure 8 shows the dependence of the bonding strength on impact velocity. It was reported previously that the bonding strength of the impact-welded bars is independent of impact velocity because a fracture has not occurred at the joining interface, but on the aluminum projectile. However, as shown in Fig. 8, the bonded strength of the tube decreases with higher impact velocities. The difference of the two tendencies depends on the following difference of the deformation processes of the bar and tube.

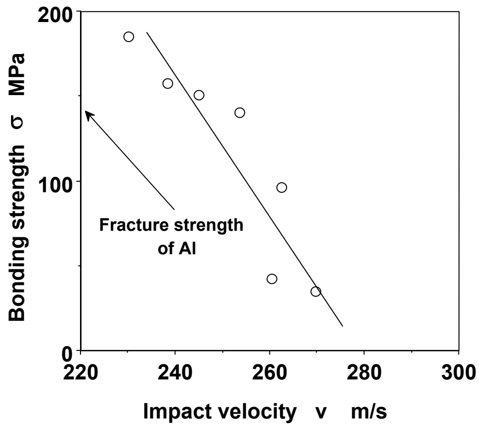

Fig. 8 Effect of impact velocity on bonding strength

The radial deformation was generated at the impact face of the cylindrical projectile subjected to a longitudinal impact. Since the radial displacement increases with the radial distance at symmetric deformation with respect to the axis, the deformation applies a shearing force on the joint. In the case of impact welding of the bar, the compound layer hardly suffers deformation because the layer was formed in the vicinity of the center. However, since the forming position of the compound layer at the impact face of the tube is near the inner wall, a shearing force acts on the interface. It is also clarified that the shearing deformation

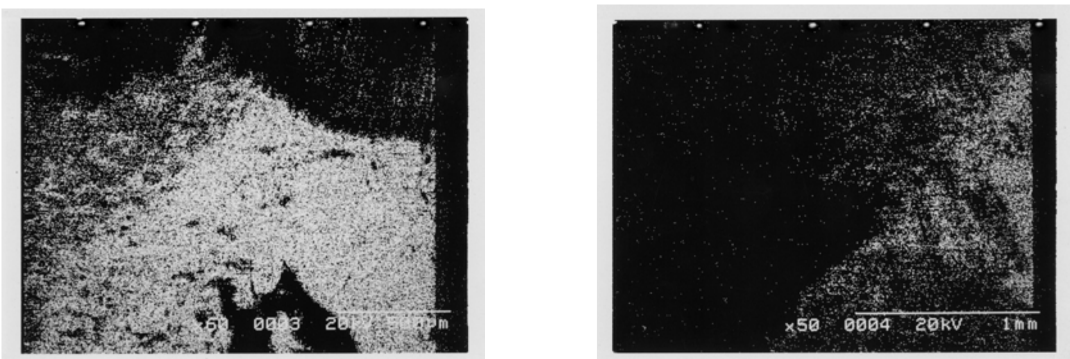

(a) v = 233 m/s (b) v = 260 m/s

Fig. 9 EDX images of fracture surface obtained by tension test increases with impact velocity. It is conjectured that the deformation initiates a micro-crack in the layer and the increasing of the impact velocity causes the length of the crack to increase. The X-ray image analyses of the fracture surface at the point with the maximum bonding strength in the compound layer after the tension test are shown in Fig. 9 (a) and (b). The impact velocities are 233 m/s and 260 m/s, respectively. Since the white dots show aluminum, a decrease of aluminum is observed with impact velocity. The decrease of aluminum indicates that the fracture surface moves from the aluminum side to the compound layer side with increasing impact velocity. Finally, when impact welding of a tube was carried out with impact velocities of 220 ~ 240 m/s, the bonding strength was stronger than the fracture strength of aluminum.

CONCLUSIONS

An aluminum tube was impact welded onto a stainless steel target and the following results were obtained.

1) Acceptable impact-welding was obtained at impact velocities from 200 m/s to 300 m/s because the inside flow of metal in the tube caused poor welding at impact velocities of 300 m/s or more.
2) Since the temperature generated at the impact face of the tube was lower than that obtained by the impact-welding of the bar, the thickness of the compound layer was thinner than that of the bar and hardly depends on impact velocity.
3) The bonding strength decreased with impact velocity because the bonding surface received shearing deformation with impact velocity.
4) The bonding strength was stronger than the fracture strength of aluminum, when impact welding of a tube was carried out at impact velocities of 230 ~ 250 m/s.

References

[1] Date H., S. Kobayakawa and M. Naka (1999) “ Microstructure and bonding strength of impact-welded aluminum-stainless steel joints”, J. Mater. Process. Technology, 55, 166-170.

[2] Date H. (1998) ” Dynamic Behaviors of Aluminum Tube Subjected to a Longitudinal Impact and Tentative Impact Welding of a Tube”, Trans. of JSME, 64, 1316-1321.

[3] Date H. and M. Naka (2000) ” Formation Mechanism of Compound layer by Impact Welding”, Proc. of PLASTICITY ’00, edited by A.S. Khan, H. Zhang and Y. Yuan, 219-221